Alzoubi *et al. Chem. Biol. Technol. Agric. (2019) 6:4*
https://doi.org/10.1186/s40538-019-0142-7

Chemical and Biological Technologies in Agriculture

RESEARCH

Open Access

Prediction of environmental indicators in land leveling using artificial intelligence techniques

Isham Alzoubi[1*], Salim Almaliki[2] and Farhad Mirzaei[3]

Abstract

Background: Land leveling is one of the most important steps in soil preparation and cultivation. Although land leveling with machines require considerable amount of energy, it delivers a suitable surface slope with minimal deterioration of the soil and damage to plants and other organisms in the soil. Notwithstanding, researchers during recent years have tried to reduce fossil fuel consumption and its deleterious side effects during this operation. The aim of this work was to determine the best linear model using Artificial Neural Network (ANN), Imperialist Competitive Algorithm–ANN, regression, and Adaptive Neural Fuzzy Inference System (ANFIS) to predict the environmental indicators for land leveling and to determine a model to estimate the dependence degree of parameters on each other.

Methods: New techniques such as ANN, ICA, GWO–ANN, PSO–ANN, sensitivity analysis, regression, and ANFIS that using them for optimizing energy consumption will lead to a noticeable improvement in the environment. In this research, effects of various soil properties such as embankment volume, soil compressibility factor, specific gravity, moisture content, slope, sand percent, and soil swelling index in energy consumption were investigated. The study was consisted of 350 samples which were collected from 175 regions in two depths. The grid size was set 20 m × 20 m from a 70-ha farmland in Karaj province of Iran.

Results: The models that reveals the relationship between the land parameters and the energy indicators were extracted. As it was expected three parameters; density, soil compressibility factor and, embankment volume index had significant effect on fuel consumption. In comparison with ANN, all ICA–ANN models had higher accuracy in prediction according to their higher R^2 value and lower RMSE value. Statistical factors of RMSE and R^2 illustrate the superiority of ICA–ANN over other methods by values about 0.02 and 0.99, respectively. Results also revealed the superiority of integrated techniques over other methods for prediction of complicated problems such as land leveling energy estimation.

Conclusion: Results were extracted and statistical analysis was performed, and RMSE as well as coefficient of determination, R^2, of the models were determined as a criterion to compare selected models. According to the results, 10-8-3-1, 10-8-2-5-1, 10-5-8-10-1, and 10-6-4-1 MLP network structures were chosen as the best arrangements and were trained using Levenberg–Marquardt as NTF. Integrating ANN and imperialist competitive algorithm (ICA–ANN) had the best performance in prediction of output parameters, i.e., energy indicators.

Keywords: Artificial Neural Network, Energy, Environmental research, Imperialist competitive algorithm, ANFIS

*Correspondence: alzoubi@ut.ac.ir; iazzabi@yahoo.com
[1] Department of Surveying and Geometric Eng, Engineering Faculty, University of Tehran, Tehran, Iran
Full list of author information is available at the end of the article

Introduction

During the last century due to increasing human population, demands for agricultural commodities have been enormously increased. Nowadays, one of the cardinal environmental challenges in the world is energy production and consumption. Despite soft growth of renewable energy usage such as solar energy, inappropriate use and lack of proper management have led to an intensive rise in fossil fuel energy consumption in this field. It also should be taken into the account that environmental conservation and market globalization will be dependent on food security in the future agriculture [1]. Regarding this, some special policies should be addressed to consider energy viewpoint in conjunction with the environmental issues to solve the problem. Land leveling is one of the heaviest and costly operations among agricultural practices that consume considerable amount of energy. In addition, moving heavy machines on the ground makes the soil denser, particularly in the wet regions where the moisture content of the soil is high and it makes a situation that is not easily recoverable [2–4]. On the other hand, land leveling simplifies the irrigation, improves field situations in other practices related to agriculture and regulates the soil surface and normalizes its slope [5]. Reportedly, there are three significant factors which have effect on grain yield including the effects of land leveling, methods of water application and the interaction between land leveling and water applied. Okasha et al. observed a noteworthy connection between slope and diverse irrigation scheme in different seasons [2]. Some researchers have used other techniques such as Internet of Things (IoT) to optimize the irrigation process based on the physical characteristics of soil [6]. However, these methods do not engage in land leveling process. Diverse methods of land leveling can affect the physical and chemical properties of the soil, and hence can make differences in plant establishment, root growth, aerial cover and eventually crop yield. As a direct result, one of the most important steps in soil preparation and a key factor in food production that should be optimized is land leveling [5]. Besides, decreasing fossil fuel consumption for land leveling diminishes air contaminants and improves the environmental condition. There is a growing understanding of importance and effects of water and soil management which in turn reveals the significance of optimized laser land leveling from social, financial and agronomic points of view [7]. Even though some improving strategies have been proposed for the enhancement of operations related to the environment, they have diverse undesirable effects [8]. Using computers and the Internet has shown a great potential to solve these types of problems by reducing the aforementioned undesirable effects. There are myriad of computer-based techniques and recently IoT that are used widely to solve engineering problems [9]. ANNs are one of these methods. ANN is a conceptual technique, the output or inferred variable of which can be modeled in terms of other parameters that are relevant to the same process [10]. This technique has been widely used in engineering field for optimization and prediction [11]. Ahmadi et al. proposed ANNs trained with Particle Swarm Optimization (PSO) and Back Propagation (BP) algorithm to estimate the equilibrium water dew point of a natural gas stream with a Triethylene Glycol (TEG) solution at different TEG concentrations and temperatures. They reported that this approach, PSO–ANN, can aid in better understanding of fluid reservoirs' behavior through simulation scenarios and statistical result was quiet noticeable [12, 13]. In another research, a feed-forward ANN optimized by PSO was used as an artificial intelligence modeling tool to predict asphalting precipitation due to natural depletion [14]. They also proposed another network based on feed-forward ANN optimized by Hybrid Genetic Algorithm and Practical Swarm Optimization (HGAPSO) and compared it with conventional BP-ANNs. They reported that results of this approach were better than conventional methods, based on statistical analysis [15]. This technique has been also used for predicting parameters with reducing uncertainties. In a research, Ahmadi et al. used artificial intelligence techniques to accurately determine the amount of Dissolved Calcium Carbonate Concentration in oil field brines with minimum uncertainty [16]. In another study, Multi-Layer Perceptron (MLP)-ANN models and Adaptive Network-Based Fuzzy Inference System (ANFIS) models were adopted to predict and simulate the groundwater level of the Lamerd plain; the required results were obtained by emphasis on higher accuracy and lower scattering for modeling ANFIS with RMSE of 0.9987 and R^2 of 0.0163 in training stage, and RMSE of 0.9753 and R^2 of 0.0694 in test stage [17]. ANN and ANFIS were also used to predict the subsurface water level in paddy fields of Plain Areas between Trajan and Nectarous Rivers. The correlation coefficient of the proposed models was 0.8416 and 0.8593 and RMSE of them were 0.2667 and 0.249, respectively [18]. Likewise, ICA is a new evolutionary algorithm in the Evolutionary Computation field based on the human's socio-political evolution. This algorithm has been proposed by Atashpaz-Gargari and Lucas in 2007 [19, 20]. It simulates an optimization problem by analogizing variables to colony and imperial countries. This method has been widely used in solving engineering problems [21] such as data clustering [22], Nash balance point attainment [23], ANNs training [15] composite constructions [24, 25], production administration complications [19], and optimization complications [26–28]. Environmental

Impact Assessment (EIA) was also addressed in literature which involves the investigation and estimation of scheduled events with a view to ensure environmentally sound and sustainable improvements [8]. Since, land leveling with machines requires considerable energy, thus, optimizing energy consumption in the leveling operation is expected. As a result, here, five approaches including ANN, integrating Artificial Neural Network and Imperialist competitive algorithm (ICA–ANN) and Sensitivity Analysis, Regression, ANFIS models have been tested and evaluated in prediction of environmental indicators for land leveling. Moreover, since a limited number of studies associated with the energy consumption in land leveling have been done, the objective of current energy and cost research is to find a function for all the indices of the land leveling including the slope, coefficient of swelling, the density of the soil, soil moisture, special weight dirt and the swelling.

Materials and methods

Case study region

To verify the accuracy and applicability of the proposed linear model, a case study was carried out based on requirements of the project in a farmland at Karaj, Iran. The farm area was 70 ha and was located in west of Karaj, 31°28′42″ north latitude and 48°53′29″ east longitude. Topographic maps of the farm were plotted at scale of 1:500. Length, width and height of points from a reference point (coordinates of x, y and z) were considered as outputs. The grid size in the case study region was 20×20 m during topography operations. Samples were collected from the canters of each grid and two different depths; surface soil (0–10 cm) and subsurface soil (10–30 cm). Totally, 350 samples (175 grid cells multiplied by 2 depths) were collected. In the laboratory, collected moist soil samples were firstly sieved through 10-mm mesh sieve to remove gravel, small stones and coarse roots and plant remnants; then passed through 2-mm sieve. Then, the sieved samples were dried at room temperature and moisture content of the samples as well as texture, bulk density, land slope and soil optimum density were determined.

Development of the ANN model

ANNs are massively parallel-distributed information processors that have certain performance characteristics resembling biological neural networks of human brain [29]. They have been developed as a generalization of mathematical models of human biological neural system [18]. There are a lot of structure types of ANN models. In this study, a typical feed-forward back propagation (BP) MLP structure was used. The main advantage of MLP structures over other types is that they have the ability to learn complex relationships between input and output patterns, which would be difficult to model with conventional algorithmic methods [30]. An ANN structure usually consists of an input layer, followed by one or more hidden layers and an output layer. The input nodes are the previous lagged observations, while the output provides the forecast for the future value. Hidden nodes with appropriate nonlinear transfer functions are used to process the information received by the input nodes. The model can be written as follows [28]:

$$y_t = \alpha_0 + \sum_{j=1}^{n} \alpha_j f\left(\sum_{i=1}^{m} \beta_{ij} y_{t-i} + \beta_{0j} + \varepsilon_t\right), \quad j = 0, 1, \ldots, n \text{ and } i = 0, 1, \ldots, m \tag{1}$$

where m is the number of input nodes, n is the number of hidden nodes, α_j denotes the vector of weights from the hidden to output nodes and β_{ij} denote the weights from the input to hidden nodes. α_0 and β_{0j} represent weights of arcs leading from the bias terms which have values always equal to 1 and f is a sigmoid transfer function [31]. Multiple layers of neurons with nonlinear transfer functions allow the network to learn nonlinear and linear relationships between input and output parameters [32]. The linear output layer lets the network to take any values even outside the range of -1 to $+1$; while if the last layer of a multilayer network has sigmoid neurons, then the outputs of the network will be only in a limited range [33]. Input variables were: specific gravity, density, moisture content, slope, inflation rate and type of the cut soil. Relevantly, output variables were: fuel energy, machinery energy, labor power, total cost and energy consumption. In this study, all available data sets were used for regression modeling, but for ANN model development, data were randomly divided into three groups: 70% for training the network, 15% for model cross validation and, 15% for testing [30]. Several architectures for type of MLP have been investigated to find the one that could result in the best overall performance. The learning rules of Momentum and Levenberg–Marquardt were considered and no transfer function for the first layer was used. For the hidden layers, the sigmoid and hyperbolic tangent transfer functions were applied, and for the last one a linear transfer function was set. Also, a number of different network sizes and learning parameters have been tried.

As it is mentioned earlier, the ANN system applied for the predictor models had seven inputs; soil cut/fill volume, soil compressibility factor, specific gravity, moisture content, slope, sand percent, and soil swelling index. On the other side, the outputs of each model were labor energy, fuel energy, total machinery cost, total machinery energy.

Since the main elements of ANNs are constituted by artificial neurons, the input model consists of dendritic nodes similar to a biological cell that could be represented as a vector with N items $X = (X_1, X_2, \ldots, X_n)$; the summation of inputs multiplied by their corresponding weights could be represented by scalar quantity S.

$$S = \sum_{k=1}^{n} W_k X_k, \tag{2}$$

where $W = (W_1, W_2, \ldots, W_N)$ is the weight vector of associations among neurons. The S quantity is then passed to a non-linear activation function f, yielding the following output:

$$y = f(s). \tag{3}$$

Non-linear transfer function is usually represented as sigmoid functions and is defined via:

$$f(s) = \frac{1}{1 + e^{-s}}. \tag{4}$$

The output of y can be the final result of the model or that of the previous layer (in multilayer networks). In the design of an ANN, certain elements should be taken into the account including type of input parameters. In this research, three-layer perceptron network was used which is composed of an input layer and an output layer plus one hidden layer of computational modes. In each layer, a number of neurons were considered which were connected to the neurons of neighboring neurons via some associations. In these networks, the effective input of each neuron was as a result of the multiplication of the outputs of the previous neurons by the weights of those neurons. Neurons in the first layer receive the input information and transfer it to hidden neurons through related connections. The input signal in such networks is only expanded in a forward direction. The main advantage of such a network is the simplicity in implementing the model and estimating input/output data. Some of the major shortcomings of this model are the low training rate and need for a huge set of data.

Imperialist competitive algorithm (ICA)

ICA is a novel swarm-intelligence method that has been developed by mimicking the human being's socio-political evolution strategies. ICA optimization process starts with initialization of random populations and some incipient empires. In each stage of ICA, a union of subgroups, colonies, and imperialists assemble the empires. ICA breaks the early population into the subpopulations, and then it searches the solution space for the best point using two main operators: competition and assimilation. During algorithm proceedings, empires can interact with the members of the swarm. Throughout the assimilation procedure, colonies move towards the relevant imperialist progressively. Imperialistic competition among the empires is the momentous procedure of the ICA [12, 19–21]. In competition stage, powerless empires collapse; whereas, the dominant ones gain further control over their colonies. This operation is stopped whenever one empire controls the entire countries. In termination condition, empire has equal cost with its colonies, which can be regarded as a satisfactory solution for the problem. To explain the algorithm more practically, the required steps are as follows: Step 1: Initializing phase. Scattering the early population randomly over the search space and composing the basic solutions in the format of a $1 \times N_{var}$ array via Eq. (5):

$$\text{country} = [p_1, p_2, p_3, \ldots, p_{N_{\text{var}}}], \tag{5}$$

where p_i represents variables that are fundamentally related to socio-political characteristics of the countries such as culture, language, religion, and economic policy. N_{var} shows the total variables of the target problem. Step 2: computing the cost of every country using Eq. (6):

$$C = f(\text{country}) = f(p_1, p_2, \ldots, p_{N\text{var}}) \tag{6}$$

Step 3: Initializing the empires. The normalized cost of an imperialist is obtained via Eq. (7)

$$\text{NC}_n = f_{\text{cost}}^{(\text{imp},n)} - \max_i \left(f_{\text{cost}}^{(\text{imp},i)} \right), \tag{7}$$

where $f_{\text{cost}}^{(\text{imp},n)}$ stands for the cost of nth imperialist, and NC_n indicates its normalized cost.

p 4: Dividing the colonies among imperialists. This process is based on the power of imperialist and relationships between the countries and their interdependent empires (i.e., the countries should be possessed by their imperialist based on the power). This step is completed using Eqs. (8–10), respectively:

$$\text{Power}_n = \left| \frac{\text{NC}_n}{\sum_{i=1}^{N_{\text{imp}}} \text{NC}_i} \right|, \tag{8}$$

$$\text{NOC}_n = \text{round}\{\text{Power}_n, N_{\text{col}}\}, \tag{9}$$

$$N_{\text{col}} = N_{\text{pop}} - N_{\text{imp}}, \tag{10}$$

where Power_n is the normalized power of each imperialist, N_{col} and N_{imp} are the given number of colonies and imperialists, respectively, and NOC_n represents the total number of colonies that are possessed by nth empire. Step 5: Assimilation strategy. The purpose of the assimilation procedure can be expressed as the movement of the colonies towards their interdependent imperialist. Based on this stage, each movement is performed according to Eq. (11):

$$x \approx U(0, \beta \times d) \quad \beta > 1, \tag{11}$$

where x is a random number with uniform (or any proper) distribution, β is a number greater than 1, and d is the distance between a colony and related imperialist. Step 6: Revolution strategy. In this strategy, a random amount of deviation is added to direct the colonies movement via Eq. (12):

$$\theta \approx U(-\gamma, \gamma) \tag{12}$$

where θ is a random variable with uniform distribution, and γ shows a parameter for adjusting the deviation from the initial movement direction. Step 7: Exchanging phase. During assimilation, whenever a colony reaches to a position with lower (better) cost compared with the imperialist, the imperialist and the colony exchange their positions, and the colony becomes new imperialist and vice versa. Step 8: Imperialistic competition phase. Calculating the overall power of an empire that is mainly affected by the power of empire and its colonies as Eq. (13):

$$\mathrm{TC}_n = f_{\mathrm{cost}}^{(\mathrm{imp},n)} + \xi \cdot \frac{\sum_{i=1}^{\mathrm{NC}_n} f_{\mathrm{cost}}^{(\mathrm{col},i)}}{\mathrm{NC}_n}, \tag{13}$$

where TC_n represents the total cost of the nth empire, and ζ is a coefficient between 0 and 1 for decreasing the effect of colonies cost. Step 9: Imperialistic competition strategy. Based on this process, each empire tries to extend its power to possess more colonies compared with other empires. Throughout the competition, weakest colony from the weakest empire is selected to be governed by the strongest empire. Imperialistic competition conducts a searching procedure towards a peak solution. The competition operator is designed to dedicate the colonies of the weakest empires to other empires. Based on TC_n, the normalized total cost is evaluated using Eq. (14):

$$\mathrm{NTC}_n = \mathrm{TC}_n - \max_i\{\mathrm{TC}_i\}, \tag{14}$$

where NTC_n is the total normalized cost of nth empire. According to NTC_n, the possession probability of each empire is computed with Eq. (15):

$$P_{pn} = \left| \frac{\mathrm{NTC}_n}{\sum_{i=1}^{N_{\mathrm{imp}}} \mathrm{NTC}_i} \right| \tag{15}$$

To find out the winner of competition with less computational effort, the vectors P, R, and D are formed via Eqs. (16, 17, 18):

$$P = [P_{P1}, P_{P2}, \ldots, P_{\mathrm{PNimp}}] \tag{16}$$

$$R = [r_1, r_2, \ldots, r_{N_{\mathrm{imp}}}]\, r_1, r_2, r_3, \ldots, r_{N_{imp}} \approx U(0,1) \tag{17}$$

$$\begin{aligned} D &= P - R = [P_R] = [D_1, D_2, \ldots, D_{N_{imp}}] \\ &= [P_{P1} - r_1, P_{P2} - r_2, \ldots, P_{P_{N_{\mathrm{imp}}}} - r_{N_{\mathrm{imp}}}], \end{aligned} \tag{18}$$

where P is the vector of possession probability of the imperialists and R represents a vector with uniformly distributed random values. Maximum index of D determines the winner empire of the competition. Step 10: Eliminating phase. When a powerless empire loses all of its controlled colonies, it should be removed from the competition. Step 11: Convergence phase. Finally, the most powerful imperialist controls all the remained colonies. In such a condition, the algorithm is stopped. These steps can be shown in an algorithmic flowchart such as Fig. 1.

Training of ANNs can be done using the ICA. For this purpose, the algorithm should be able to adjust the weights and bias, so that the difference between the output of ICA and real output be minimized. Mean squared error (MSE) was considered to determine the error.

Integrating Imperialist competitive algorithm and Artificial Neural Network (ICA–ANN)

In this study, after applying commands of ANNs in MATLAB software, the number of neurons in the input layer considered the same as the number of effective parameters: Cut-Fill Volume (V) (embankment volume), soil compressibility factor, specific gravity, moisture content, slope, sand percent, and soil swelling index. Similarly, the number of neurons in the output layer should be equal to the number of desired parameters for modeling. Instead of the default commands for network training, ICA was used. For running ANNs, 70% of the data were used for training, 15% for evaluation, and the remained 15% were used for the test section.

Results

Sensitivity analysis model

The outputs that are shown in Table 1 are the results of the model after running for 500 times. Table 1 indicates meaningful F-values and a great significance ($\alpha < 0.0001$) for all developed sensitivity analysis models that reject the null hypothesis clearly.

Figure 2 shows the sensitivity analysis for labor energy (LE). In this figure, F1–F7 represent land slope, moisture content, density, soil compressibility factor, embankment volume, Soil Swelling Index, and sand percent, respectively. The results revealed that F3 (density), F4 (soil compressibility factor), and F5 (embankment volume) had the highest sensitivities on LE.

Sensitivity analysis also showed that three soil parameters including; volume of soil, specific gravity and soil compaction had the greatest impact on the amount of energy required for land leveling. These parameters had direct relation with the required energy. In other words, more density of the soil leads to more required energy for constant volume of the soil. For a soil with higher densities, in addition to its weight, handling it also requires more energy consumption. It is obvious that more working time of the machine leads to higher energy consumptions. In the same manner, the higher the excavation volume, the greater the energy consumption. It can be interpreted in this way that more soil volume needs more time of machine and leads to more fuel consumption. Table 1 shows that soil volume is the most important parameter between all input variables for energy consumption including LE, FE, TMC and TME. It is clear that by increasing cut soil volume, needed time of machinery used increases, and consequently fuel energy increases as well. Furthermore, prolonged working time of machinery increases labor requirement for operation which in turn raises the energy consumption by the labors. On the other hand by decreasing the cut soil volume, required human labor also decreases. Therefore, one of the most important ways for decreasing energy consumption is to reduce soil cut/fill. In addition, in each table, if the *F* value of a variable is higher than others, it indicates the higher impact of that variable in the final model. This situation has occurred for cut-fill volume as a variable which is the most effective factor and affects all responses of interest. In the same manner, the lower F value of a variable indicates lower impact of that variable on responses.

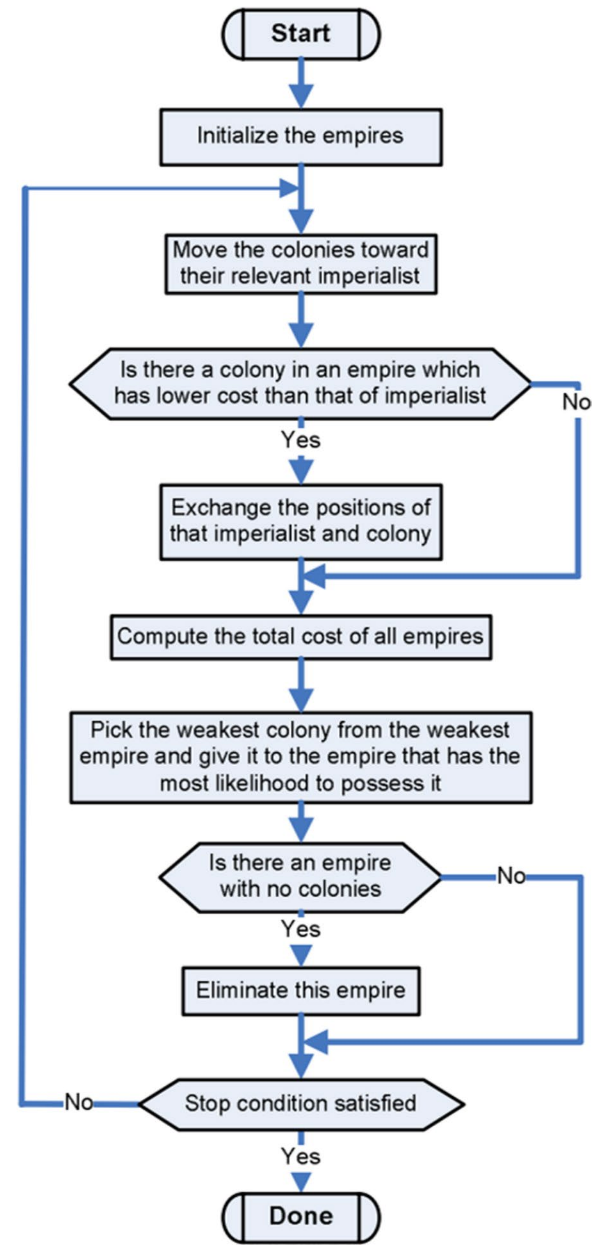

Fig. 1 Flowchart of ICA algorithm

Regression model

Since the *F*-values of all models, that are shown in Table 2, indicated a great significance ($\alpha < 0.0001$) for all developed regression models, the null hypothesis has rejected. Likewise, all models have significant *P* values as well.

Of the seven parameters of soil and land characteristics (moisture, density, soil compressibility factor, land slope, soil type, embankment volume), two factors: embankment volume and soil compressibility have the most significant effect on LE in land leveling. The factors of slope, V and soil type (sand) have significant effects on FE. V, soil compressibility factor and slope have significant effects on TMC in land leveling (Table 2).

Moreover, the results show that the effect of the land slope, swelling coefficient and soil type on energy consumption in land leveling is significant. By increasing land slope, volume of excavation and embankment increases and the number of sweep and distance traveled by leveling machines also increases and fuel consumption will increase which is obvious. Increase in soil swelling factor increases the volume of the embankment and increase in volume of the embankment also increases the demand of fuel and energy. The fitted nonlinear equations for the all response of interest including LE, FE, TMC, and TME are represented in Eqs. 19–22, respectively, in which the coefficients are provided in coded units. The coded equation is more easily interpreted. The coefficients in the actual equation compensate for

Table 1 Analysis of variance for labor energy (LE), fuel energy (FE), total machinery cost (TMC), total machinery energy (TME)

Model	Source	Sum of squares	*df*	Mean square	*F* value	*P* value Prob > *F*
LE model	Model	2.858^7	1	2.858^7	4277.61	< 0.0001
	Cut-fill volume (V)	2.858^7	1	2.858^7	4277.61	< 0.0001
FE model	Model	6.478^8	1	6.478^8	3931.00	< 0.0001
	Cut-fill volume (V)	6.478^8	1	6.478^8	3931.00	< 0.0001
TMC model	Model	2.737^{12}	1	2.737^{12}	4023.17	< 0.0001
	Cut-fill volume (V)	2.737^{12}	1	2.737^{12}	4023.17	< 0.0001
TME model	Model	1.086^{11}	1	1.086^{11}	4311.77	< 0.0001
	Cut-fill volume (V)	1.086^{11}	1	1.086^{11}	4311.77	< 0.0001

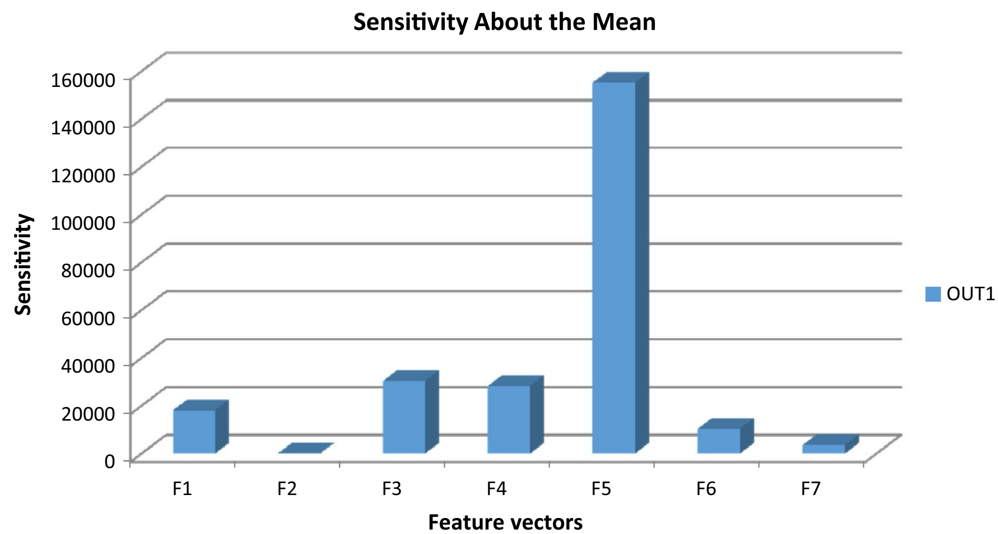

Fig. 2 Sensitivity analysis for labor energy (LE), fuel energy (FE), total machinery cost (TMC), total machinery energy (TME)

the differences in the ranges of the factors as well as the differences in the effects. Finally, LE, TMC, and TME were affected significantly only by three variables including: land slope, volume of the embankment (V), and soil swelling index (SSI). For FE model, the effect of SSI is not significant; however, soil percent has taken its place and affects the FE significantly. Labor energy consumption in land leveling is a nonlinear function of the soil compressibility factor and slope (Eq. 19). In the same way, fuel energy consumption in land leveling is also a nonlinear function of the soil compressibility factor and slope (Eq. 20). This is true for TMC and TME as well which have been represented in Eqs. 21 and 22, respectively. The value of each coefficient variable in the equation represents the effect of variable on the function.

$$(\mathrm{LE})0.8 = 34{,}161.36 + 3639.90 * \mathrm{Slope} + 31{,}173.94 * \mathrm{V} + 911.96 * \mathrm{SSI} \tag{19}$$

$$(\mathrm{FE})0.8 = 4.148^5 + 49{,}590.44 * \mathrm{Slope} + 3.782^5 * \mathrm{V} - 10{,}008.33 * \mathrm{Sand} \tag{20}$$

$$(\mathrm{TMC})0.8 = 3.319^8 + 3.587^7 * \mathrm{Slope} + 3.015^8 * \mathrm{V} + 8.393^6 * \mathrm{SSI} \tag{21}$$

$$(\mathrm{TME})0.8 = 2.494^7 + 2.621^6 * \mathrm{Slope} + 2.277^7 * \mathrm{V} + 6.787^5 * \mathrm{SSI} \tag{22}$$

A relatively flat line shows insensitivity to change in that particular factor. The response trace plot for the LE, FE, TMC and TME was sketched. At this plot, the vertical axis is the predicted values and the horizontal axis is the incremental change made in factors included in the final equation model. The scatter plots of actual values of response of interest vs. predicted values using final models are displayed in Fig. 3a, b. The strong nonlinear

Table 2 Analysis of variance for labor energy (LE), fuel energy (FE), total machinery cost (TMC), total machinery energy (TME) models

Model	Source	Sum of squares	*df*	Mean square	*F* value	*P* value Prob > *F*
LE model	Model	1.24^{11}	3	4.15^{10}	5523.914	< 0.0001
	Slope	1.85^{9}	1	1.85^{9}	246.7733	< 0.0001
	Cut-fill volume (V)	1.21^{11}	1	1.21^{11}	16,149.7	< 0.0001
	Soil swelling index (SSI)	2.61^{8}	1	2.61^{8}	34.70285	< 0.0001
FE model	Model	1.84^{13}	3	6.15^{12}	4632.446458	< 0.0001
	Slope	3.43^{11}	1	3.43^{11}	258.640572	< 0.0001
	V	1.78^{13}	1	1.78^{13}	13,457.37208	< 0.0001
	% Sand	3.28^{10}	1	3.28^{10}	24.73922519	< 0.0001
TMC model	Model	1.16^{19}	3	3.88^{18}	4751.319	< 0.0001
	Slope	1.8^{17}	1	1.8^{17}	220.2573	< 0.0001
	V	1.13^{19}	1	1.13^{19}	13,881.29	< 0.0001
	SSI	2.21^{16}	1	2.21^{16}	27.00684	< 0.0001
TME model	Model	6.64^{16}	3	2.21^{16}	5653.467	< 0.0001
	Slope	9.6^{14}	1	9.6^{14}	245.4494	< 0.0001
	V	6.47^{16}	1	6.47^{16}	16,537.35	< 0.0001
	SSI	1.44^{14}	1	1.44^{14}	36.87527	< 0.0001

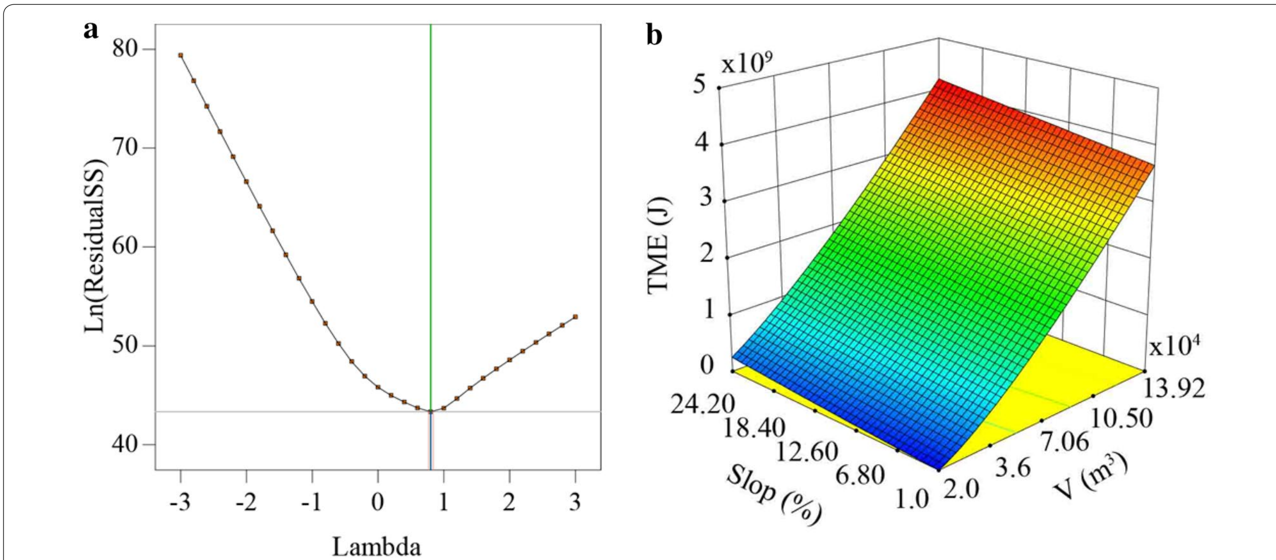

Fig. 3 **a** Box–Cox **b** surface plot of total machines energy versus slope and volume

effect of cut-fill volume on all the responses of interest is conspicuous (Fig. 3a, b). Figure 4 shows that energy and cost direct relationship with cut-fill volume as the major effect. All responses of interest are moderately affected by slope. Additionally, it is perceived that the increase of the slope led to increased energy and cost. The most appropriate power transformation (lambda) for responses is detected by the Box–Cox diagram that results the minimum residual sum of squares in the transformed model (Fig. 3a). Scatter plots of actual vs. predicted values for regression model are shown in Fig. 4a–d.

Results of ANFIS model prediction

In this section, the results of ANFIS models for prediction of LE, FE, TMC, and TME are presented. MATLAB programming language was used for implementing ANFIS simulations. Different ANFIS structures were tried using the programming code and the appropriate representations were determined. Each structure for correspond combination has been evaluated using 100 independent runs and the statistical criteria (R^2 and MSE) of the output models have been calculated for responses of interest. In Tables 3 and 4 the minimum, average and

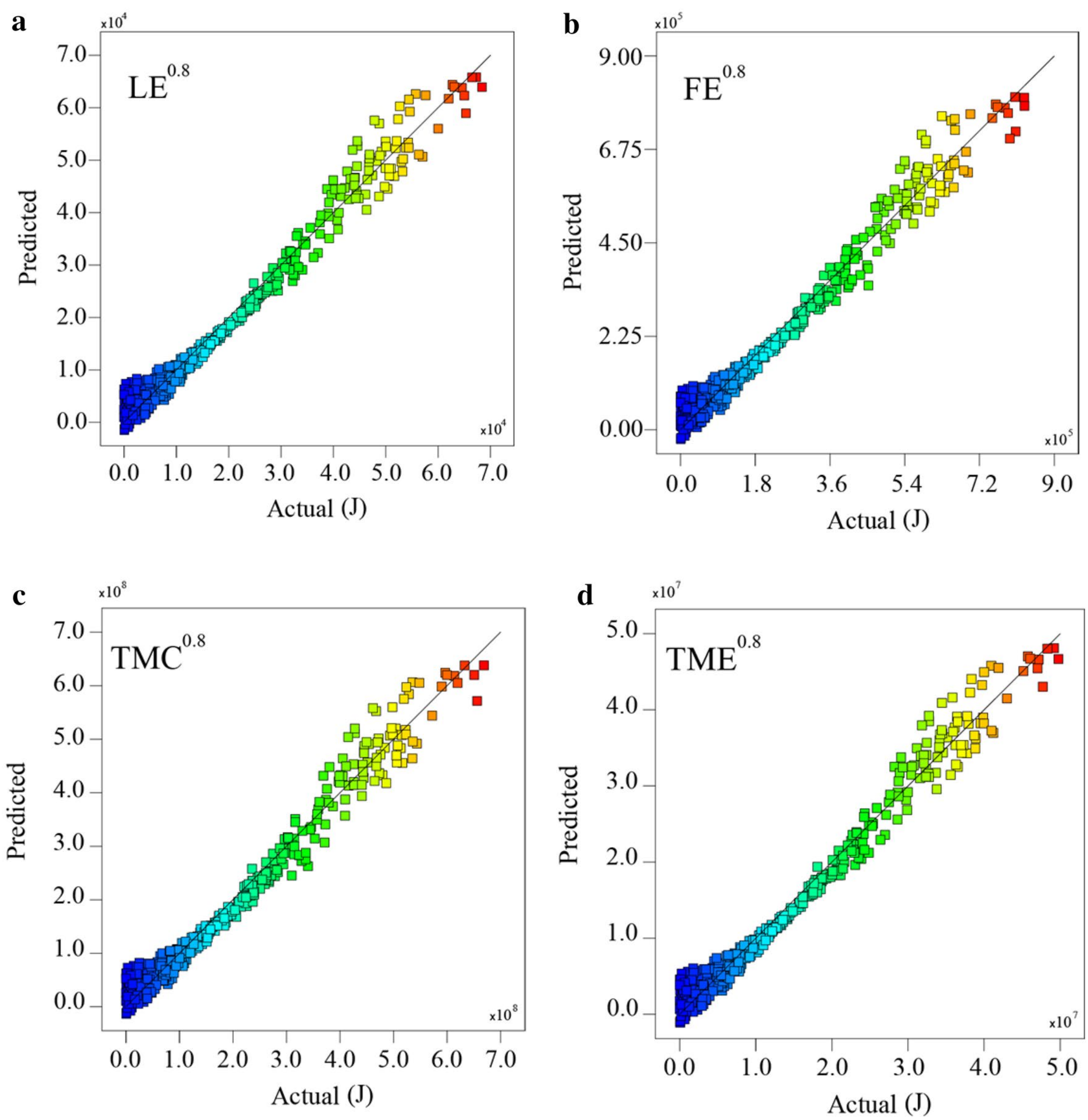

Fig. 4 Scatter plots of actual vs. predicted using regression models for **a** labor energy, **b** fuel energy, **c** total machines cost, and **d** total machines energy

maximum values of R^2 and MSE for various combinations of developed ANFIS-based models are presented. Additionally, calculated R^2 and MSE values of different developed models of labor energy vs. number of clusters are illustrated as well. It is worthwhile to mention that other outputs had similar behaviour. As presented in Table 3, statistical criteria for prediction of LE reveal that FIS model is superior to ANN-back propagation model. Average R^2 value in FIS model for prediction of LE was found to be 0.9948 and 0.9944 in Mamdani and Sugeno models, respectively; while in back propagation model, it was calculated as 0.9921. Moreover, as presented in Table 3, statistical criteria for prediction of FE reveal that FIS model are superior to ANN-back propagation model. Average R^2 value in FIS model for prediction of fuel energy was found to be 0.9927 and 0.9922 in Mamdani and Sugeno models, respectively. While in back propagation model, R^2 value was calculated as 0.9891 and 0.9892, respectively.

As presented in Table 4, statistical criteria for prediction of total machinery cost reveals that FIS model are superior to ANN-back propagation model. Average R^2

Table 3 Calculated statistical criteria for prediction of labor energy using/fuel energy different combination of optimization methods and FIS types

Optimization method	FIS type	MSE			R^2		
		Min.	Ave.	Max.	Min.	Ave.	Max.
Labor E.							
Hybrid	Mamdani	0.00063	0.00130	0.00329	0.9856	0.9948	0.9971
	Sugeno	0.00058	0.00126	0.00326	0.9865	0.9944	0.9974
Back propagation	Mamdani	0.00083	0.00102	0.00412	0.9831	0.9921	0.9965
	Sugeno	0.00088	0.00154	0.00407	0.9831	0.9921	0.9964
Fuel E.							
Hybrid	Mamdani	0.00119	0.00181	0.00371	0.9851	0.9927	0.9952
	Sugeno	0.00111	0.00173	0.00390	0.9843	0.9922	0.9955
Back propagation	Mamdani	0.00119	0.00270	0.00560	0.9775	0.9891	0.9952
	Sugeno	0.00123	0.00268	0.00560	0.9775	0.9892	0.9950

Table 4 Calculated statistical criteria for prediction of total machinery cost/energy using different combination of optimization methods and FIS types

Optimization method	Fis type	MSE			R^2		
		Min.	Ave.	Max.	Min.	Ave.	Max.
Cost							
Hybrid	Mamdani	0.00122	0.00188	0.00387	0.9837	0.9921	0.9949
	Sugeno	0.00119	0.00185	0.00394	0.9834	0.9922	0.9950
Back propagation	Mamdani	0.00140	0.00251	0.00465	0.9805	0.9894	0.9941
	Sugeno	0.00141	0.00250	0.00465	0.9805	0.9895	0.9940
Energy							
Hybrid	Mamdani	0.00059	0.00121	0.00353	0.9856	0.9950	0.9975
	Sugeno	0.00058	0.00120	0.00356	0.9855	0.9952	0.9976
Back propagation	Mamdani	0.00077	0.00183	0.00395	0.9839	0.9925	0.9968
	Sugeno	0.00080	0.00182	0.00395	0.9839	0.9926	0.9967

value in FIS model for prediction of total machinery cost was found to be 0.9921 and 0.9922 in Mamdani and Sugeno models, respectively. While in back propagation model, R^2 value was calculated as 0.9894 and 0.9895, respectively. As presented in Table 4, statistical factors for prediction of TMC indicate that FIS model perform better than ANN-back propagation model. Average R^2 value in FIS model for prediction of TME was found to be 0.9950 and 0.9952 in Mamdani and Sugeno models, respectively; while in back propagation model, it was calculated as 0.9925 and 0.9926, respectively.

Determining the effect of number of clusters on all the developed models is feasible (Fig. 5). Moreover, comparison between different optimization methods and FIS types can also be done. For the ANFIS-based model, in both training methods, the MSE (R^2) value decreases (increases) and the prediction performance of developed ANFIS-based models improves gradually with the number of clusters. In addition, comparison of the results indicates that the Hybrid method has a higher value of R^2 and a lower value of MSE; so that its results are more accurate. Also, the performance of the Sugeno FIS type was found to be better than that of Mamdani.

Comparison results of the predicted values of ANFIS models with actual data are shown in Fig. 6a–d. These predicted values are compared with actual data to show the performance of the ANFIS models for prediction of each response. Results from these figures reveal that FIS model is superior to ANN model in predicting LE, FE, TMC, and TME.

ANN model

The results of regression models and training various networks with different structures are presented in this section. The ANN models were developed by training the networks with various combination of Network Training

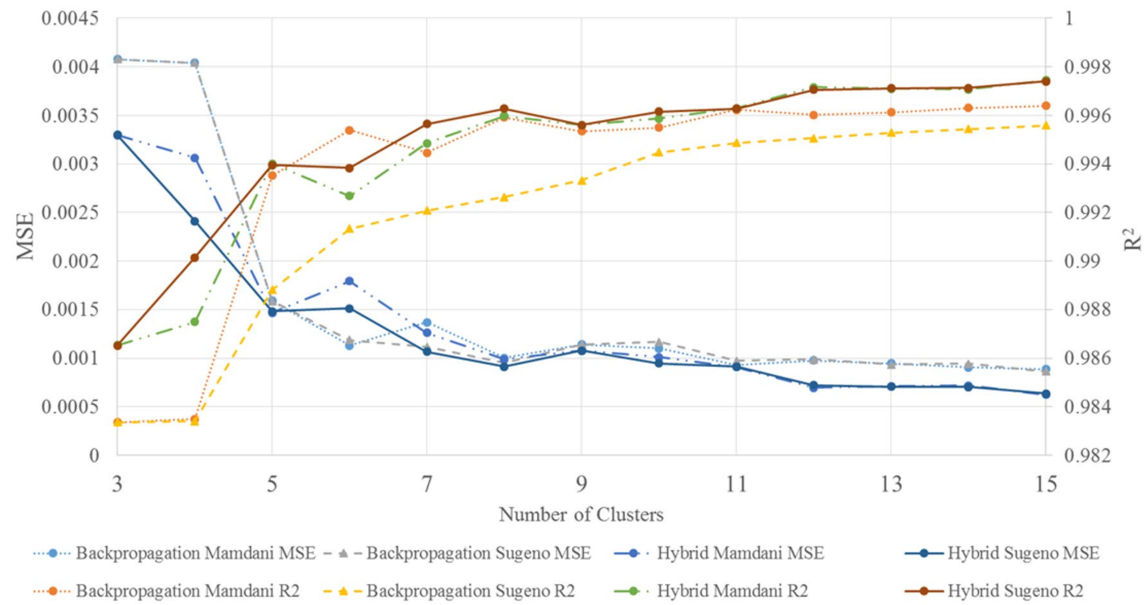

Fig. 5 Statistical performance criteria of LE

Functions (NTF), number of hidden layers and number of neurons in the each hidden layer. For selecting the best network topology, totally 20,678 different ANN models were evaluated, and the RMSE and coefficient of determination (R^2) values were calculated. For a full comparison between the performances of the trained structures, Tables 5 and 6 represent results obtained from ANN of feed-forward BP type with 7 different network training algorithms. These methods of training are available in the Neural Network Toolbox software and they use gradient- or Jacobian-based methods including Levenberg–Marquardt (trainlm), Bayesian regularization (trainbr), scaled conjugate gradient (trainscg), resilient BP (trainrp), gradient descent with momentum and adaptive learning rate BP (traingdx), Gradient descent with adaptive learning rate BP (traingda), gradient descent with momentum BP (traingdm) and conjugate gradient function (traincgf). These networks use 10 input data in the input layer to predict the outputs and utilize a linear function in their output layer to transfer the data to the output. The outputs of the model represented in Tables 2 and 3 are the results of 500 thousand runs of the model. The selected NTFs for LE in land leveling, as shown in the first row of the Table 5, were the best because they had the highest correlation coefficient and lowest RMSE. These functions had 8 neurons in the first layer, and three neurons in the second. Details of the best trained networks for prediction of LE are shown in Table 5. The NTF of trainlm had higher RMSE and lower R^2 for 2 (8-3) and 3 (2-7-6) hidden layers but NTF of trainbr for 1 hidden layer had the best statistical interpretation. The NTF of trainlm including 2 neurons in one hidden layer is the simplest ANN for forecasting the LE with RMSE lower than 0.021 and R^2 higher than 0.996. Details of the selected networks for prediction of FE are presented in Table 5. The NTF of trainlm had higher RMSE and lower R^2 for 2 (4-2) and 3 (8-2-5) hidden layers but NTF of trainscg for 1 hidden layer had the best statistical output. The NTF of trainlm including 2 neurons in one hidden layer was the simplest ANN for predicting the FE with RMSE of lower than 0.033 and R^2 higher than 0.995. As it is shown in the Table 6, the first model consisting of three hidden layers (5-8-10 topology) had the highest coefficient of determination (0.9966) and the lowest values of RMSE (0.0287) indicating that this model can predict the TMC accurately. So, this model was selected as the best solution for estimating the TMC. The detail of the selected networks for prediction of TME is presented in Table 6. The NTF of trainlm had higher RMSE and lower R^2 for 2 (6-4) and 3 (4-5-3) hidden layers. However, NTF of trainscg for 1 hidden layer had the best statistical results. For forecasting the FE, the NTF of traingdx including 2 neurons in one hidden layer was the simplest ANN. The RMSE for this model was found to be 0.225 which was very low.

ANN Models shown in the Fig. 7. This figure shows the actual responses versus the predicted ones. As the predicted values come closer to the actual values, the points on the scatterplot come closer to the diagonal line which is the regression result. Closeness of the points to the line is an evidence of satisfactory performance of the

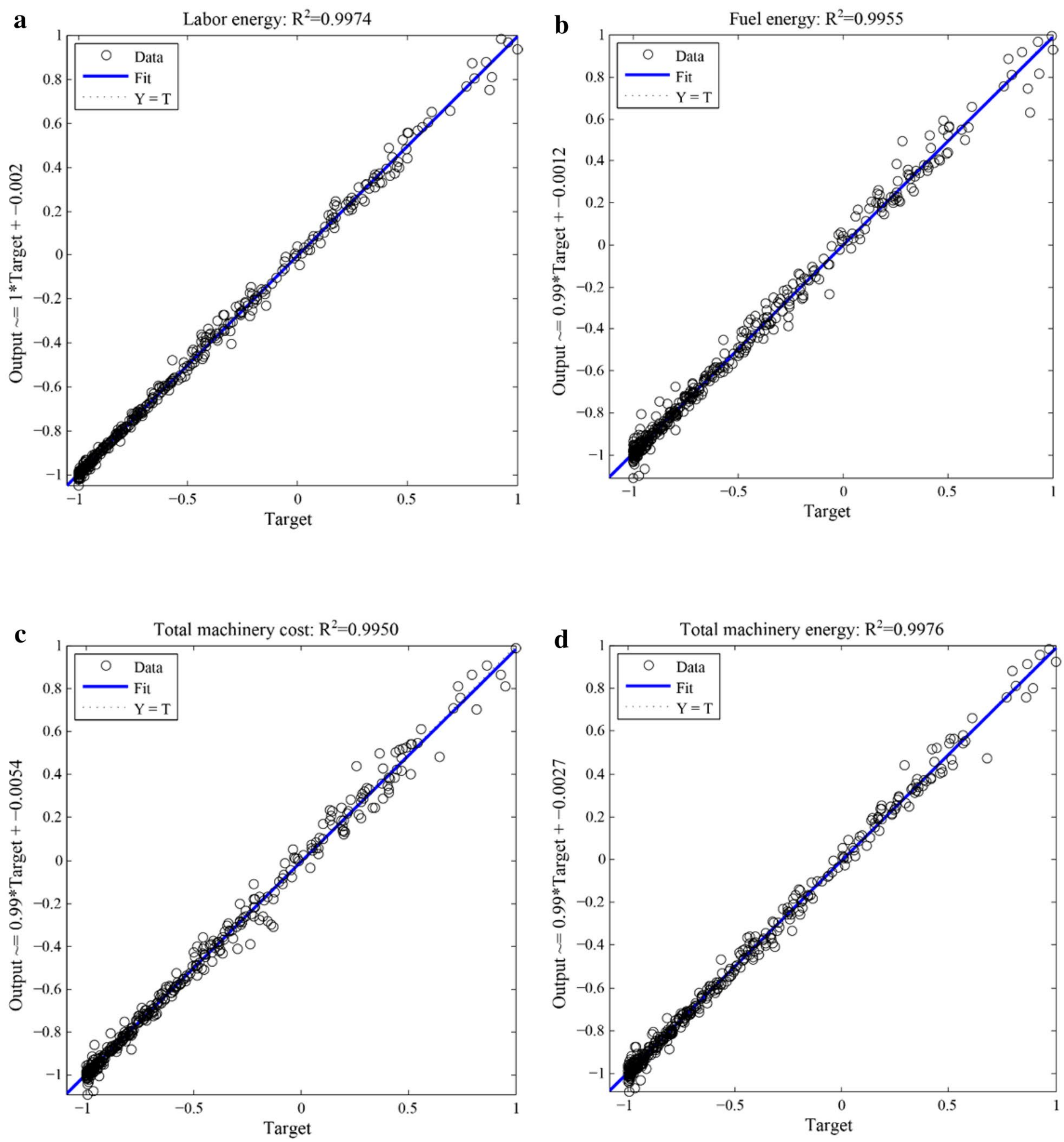

Fig. 6 Scatter plot for the predicted model and actual values of **a** labor energy, **b** fuel energy, **c** total machinery cost, **d** total machinery energy

models in prediction of the targets. For a perfect fit, the data should fall along a 45-degree line, where the network outputs are equal to the targets. The training record was used to plot the training, validation, and test performance of the training progress (error vs. number of training epochs).

Integrating Artificial Neural Network and Imperialist competitive algorithm (ICA–ANN) model

The results of training various networks with different structures are presented in this section. By training the networks with different number of neurons (3–11) in the hidden layer using ICA with parameters presented in Table 7, the ANN models were developed. For

Table 5 Selected ANN for prediction of labor energy (LE), fuel energy (FE)

Selected ANN for prediction of labor energy (LE)				Selected ANN for prediction of fuel energy (FE)			
NTF	Network topology	RMSE	R^2	NTF	Network topology	RMSE	R^2
trainlm	8-3	0.0159	0.9990	trainlm	8-2-5	0.0206	0.9983
trainlm	4-9	0.0159	0.9990	trainlm	10-4-10	0.0224	0.9980
trainlm	2-7-6	0.0164	0.9989	trainlm	4-2	0.0238	0.9977
trainlm	7-10	0.0164	0.9989	trainlm	9-2-3	0.0241	0.9977
trainlm	5-3	0.0165	0.9989	trainlm	5-2-9	0.0248	0.9976
trainlm	9-5-6	0.0166	0.9989	trainlm	3-2	0.0253	0.9974
trainlm	6-2-3	0.0167	0.9989	trainlm	2-2-2	0.0269	0.9971
trainlm	7-2-3	0.0171	0.9988	trainlm	2-2	0.0271	0.9971
trainbr	3-2	0.0174	0.9988	trainbr	2-6	0.0279	0.9969
trainbr	10-7	0.0179	0.9987	trainlm	6-2-2	0.0310	0.9962
trainbr	4	0.0171	0.9988	trainbr	5	0.0249	0.9975
trainlm	2	0.0209	0.9982	trainlm	6	0.0255	0.9980
traincg	6	0.0217	0.9981	trainscg	11	0.0261	0.9973
trainrp	7	0.0254	0.9974	traingdx	3	0.0329	0.9957
traingdx	2	0.0298	0.9964				

Table 6 Selected ANN for prediction of total machinery cost (TMC), total machinery energy (TME)

Selected ANN for prediction of total machinery cost (TMC)				Selected ANN for prediction of total machinery energy (TME)			
NTF	Network topology	RMSE	R^2	NTF	Network topology	RMSE	R^2
trainlm	5-8-10	0.0287	0.9966	trainlm	6-4	0.0157	0.9990
trainlm	7-9-2	0.0298	0.9963	trainlm	4-5-3	0.0158	0.9990
trainlm	4-5-7	0.0304	0.9961	trainlm	6-2-4	0.0160	0.9990
trainlm	7-8	0.0329	0.9957	trainlm	2-7	0.0163	0.9989
trainlm	7-2-2	0.0332	0.9954	trainlm	3-2	0.0164	0.9989
trainlm	3-2-3	0.0332	0.9954	trainbr	5-6	0.0167	0.9989
trainlm	2-4-10	0.0343	0.9951	trainlm	3-2-8	0.0168	0.9989
trainlm	2-2-5	0.0345	0.9951	trainlm	9-2-10	0.0171	0.9989
trainbr	3-9	0.0345	0.9950	trainlm	2-4-2	0.0192	0.9985
trainbr	5-8	0.0349	0.9950	trainlm	2-2-2	0.0199	0.9984
trainscg	7	0.0321	0.9958	trainscg	8	0.0164	0.9989
trainlm	2	0.0325	0.9948	trainlm	3	0.0176	0.9987
trainbr	5	0.0328	0.9955	traingdx	2	0.0300	0.9964
trainrp	4	0.0368	0.9944				
traingdx	2	0.0433	0.9922				

each response totally 18,000 networks were trained and evaluated. After several repetitions, the RMSE and coefficient of determination (R^2) values were calculated. The network utilized a tansig function in its output layer to transfer the data to the output. The results obtained from the best trained models and their characteristics are illustrated in Table 8. R^2 value for prediction of LE was found to be 0.9987 and FE was predicted by R^2 value of 0.9975. Using a network topology of 2-layer structure, TMC was predicted by R^2 value of 0.9963. While, R^2 value for prediction of TME was found to be 0.9987. Scatter plots of Actual versus Predicted results of the ANN Models are shown in Fig. 8a–d. As the predicted values come closer to the actual values, the points on the scatterplot fall closer around the regression result (the diagonal line). These models can predict the target accurately and that is evident from closeness of the points to the line. For a perfect fit, the data should fall along a 45-degree line,

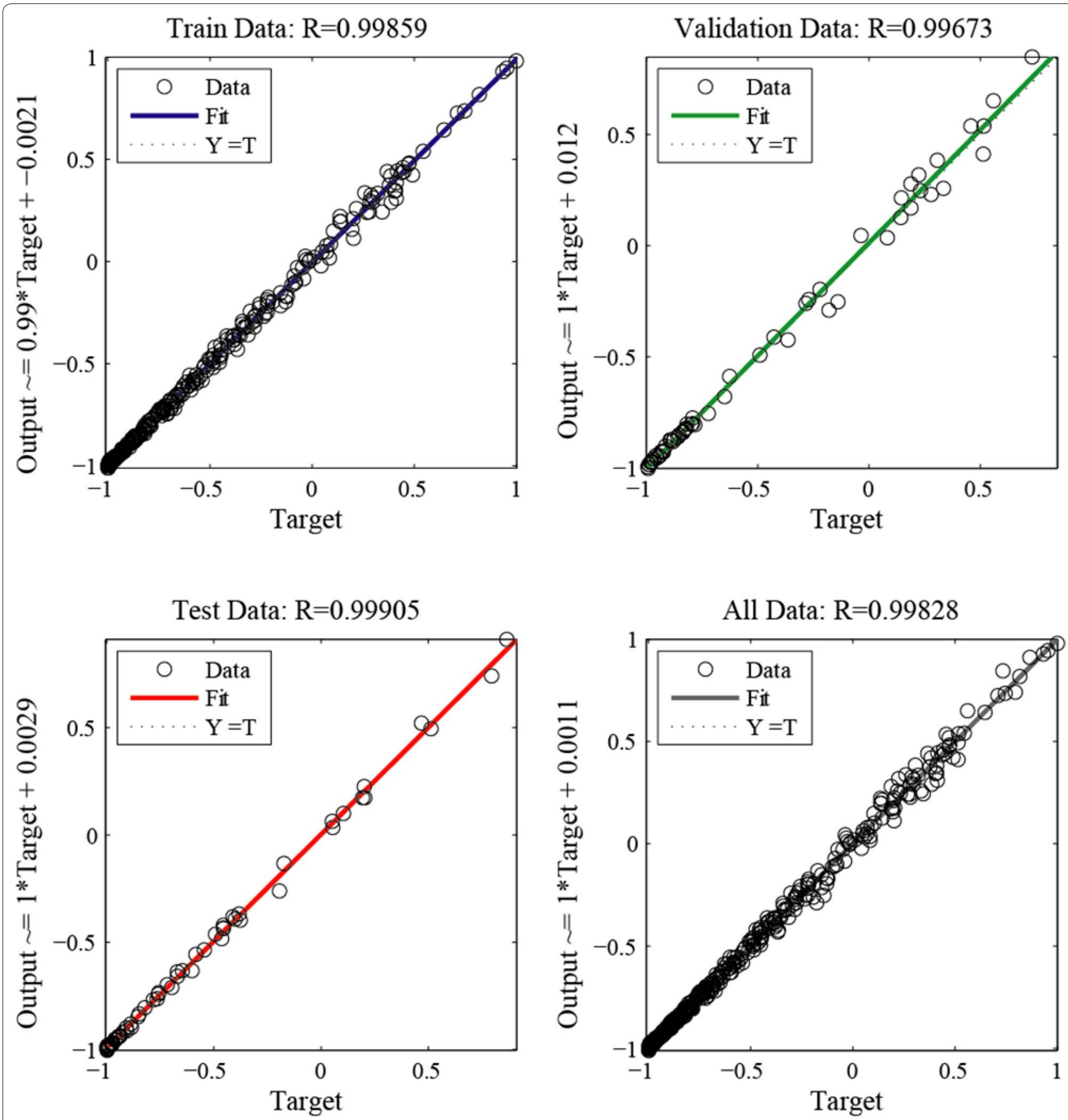

Fig. 7 Scatter plots of output vs. target using ANN models for prediction of LE

where the network outputs are equal to the actual data. Figure 8a shows the scatter plot of output data versus actual data using ICA–ANN models for prediction of LE. It is clear that the predicted outputs are very close to the target values. Figure 8b is related to the scatter plot of the output data in contrast with target data using ICA–ANN models for prediction of FE. It is also evident for the FE values that the predicted results are very close to the target values. Figure 8c illustrates the scatter plot of output in comparison with target using ICA–ANN models for prediction of TMC. This figure clearly demonstrates that the predicted TMC values are very close to the target values. The scatter plot of output vs. target values for TME is presented in Fig. 8d. As it is evident, the predicted TME values are approximately fitting to the target

Table 7 Algorithm parameters

Algorithm parameter	Value
Number of countries	250
Number of initial imperialists	25
Number of decades	500
Revolution rate	0.3
Assimilation coefficient	2
Assimilation angle coefficient	0.5
Zeta	0.02
Damp ratio	0.99
Uniting threshold	0.02

values. By and large, the results show good performance of ICA–ANN to predict LE, FE, TMC, and TME.

As shown in (Fig. 8), among four applied methods to predict LE, FE, TMC, and TME according to three selected input parameters (soil cut/fill volume, specific gravity, and soil compressibility factor), RMSE of LE and TME was less than that of FE and TMC. In fact, using ANN-based prediction methods (ANN, ICP–ANN, PSO–ANN and GA–ANN) were predicted LE and TME more accurately than FE and TMC. On the other hand, as it is evident in (Fig. 8b), R^2 of prediction of LE and TME was higher than that of LE and TME.

According to the comparison of R^2 between four ANN methods, it is revealed that among these methods, GA–ANN had the maximum R^2 value in prediction of TME, FE, and TMC. It is noticeable that the R^2 value of LE, resulted from GA–ANN, was less than other algorithms.

On the other hand, as it is shown in Fig. 8b, the R^2 of TMC using ANN algorithm was the least value among the four mentioned algorithms. Figure 8a shows the RMSE value of all methods. As it is shown in this diagram, the ANN algorithm had the maximum RMSE value among all methods. It is obvious that a smaller R^2 and higher RMSE value will lead to worse results in the prediction. Results show that although the output values were acceptable by applying these four methods, it should be considered that ANN algorithm was the weakest algorithm for prediction of TMC as the neural networks were run 1000 times. Although GA–ANN had the best performance in prediction of TME, FE, and TMC, ICP–ANN was also a good prediction method regardless of its weakness in prediction of FE.

To compare the robustness of the proposed methods, a regression analysis with SPSS and Minitab software was conducted, and the RMSE and R^2 of the models were extracted. As it is shown in the Fig. 9 the RMSE values extracted with SPSS were greater than that of ANN, ICA–ANN, PSO–ANN, and Grey Wolf Optimizer (GWO–ANN). As it is shown in (Fig. 9), the R^2 value extracted with Minitab software was less than other methods except sensitivity analysis. The R^2 of the regression equation evaluated with SPSS software was almost equal to four ANN methods evaluated with Matlab software. It is worthwhile to mention that R^2 and RMSE are two factors by which judgments about robustness of methods were made. Higher R^2 values, and on the other hand lower RMSE values, will result in better equation coefficients; thus, as explained, these characteristics were observed in GWO. On the other hand, as it is evident from (Fig. 9a, b), the regression extracted with Minitab software had greater RMSE value and less R^2 value which results in an equation with less precision in determination of LE, FE, TMC and TMC. About the precision of SPSS software, although the R^2 value was higher than that of Minitab software and sensitivity analysis and in fact near the ANN values (Fig. 9), its RMSE was higher than that of ANN-based prediction algorithms which indicates the superiority of ANN-based methods.

Utilizing ICA–ANN for these types of optimization problems are broadly reported in engineering and the researchers acknowledged the superiority of ICA–ANN over conventional approaches. Taghavifar et al. were used a meta-heuristic optimization algorithm for prediction of soil compaction indices. ANN trials were developed and then merged with the evolutionary optimization technique of ICA. The results were compared on the basis of a modified performance function (MSE-REG) and coefficient of determination

Table 8 Comparison of integrating artificial neural network and imperialist competitive algorithm (ICA–ANN) and ANFIS and regression and ANN and sensitivity analysis models

Response	Sensitivity analysis		Regression		ICA–ANN		ANFIS		ANN	
	RMSE	R^2	RMSE	R^2	RMSE	R^2	RMSE	R^2	RMSE	R^2
LE	0.1899	0.8631	0.1394	0.9008	0.0146	0.9987	0.0159	0.9990	0.0159	0.9990
FE	0.1971	0.8562	0.1514	0.8913	0.0322	0.9975	0.0206	0.9983	0.0206	0.9983
TMC	0.1946	0.8581	0.1492	0.9128	0.0248	0.9963	0.0287	0.9966	0.0287	0.9966
TME	0.1892	0.8437	0.1378	0.9103	0.0161	0.9987	0.0157	0.9990	0.0157	0.9990

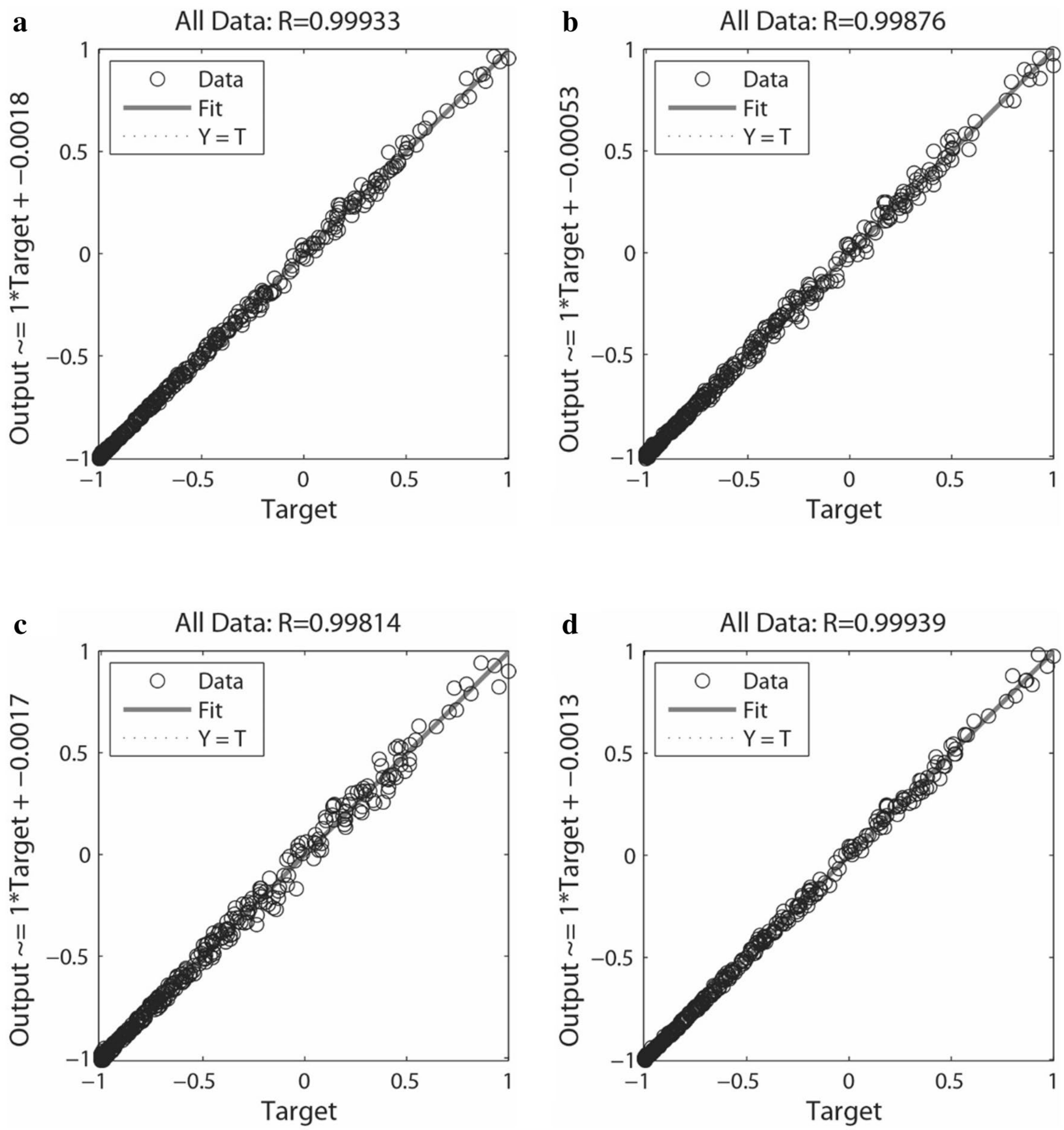

Fig. 8 Scatter plot of output vs. target using ICA–ANN models for prediction of **a** LE, **b** FE, **c** TMC, and **d** TME

(R^2). Their results elucidated that hybrid ICA–ANN succeeded to denote lower modeling error than other methods [15]. In another study, Marto et al. applied ICA–ANN for prediction of flyrock induced by blasting and parameters of 113 blasting operations were accurately recorded. The results were clearly illustrated the superiority of the proposed ICA–ANN model in comparison with the proposed BP-ANN model and empirical approaches [31]. Nikoo et al. used ICA–ANN to predict the flood-routing problem. The results proved that using this technique on flood-routing problem is a valid approach, which is not only simple but also reliable [33].

Discussion

Comparison of models

The comparison of statistical results of ICA–ANN, ANN, sensitivity analysis, regression and ANFIS models are tabulated in Table 8. As it can be seen from Table 8, among the ICA–ANN models, ANN models, Sensitivity analysis, ANFIS, and Regression, ICA–ANN

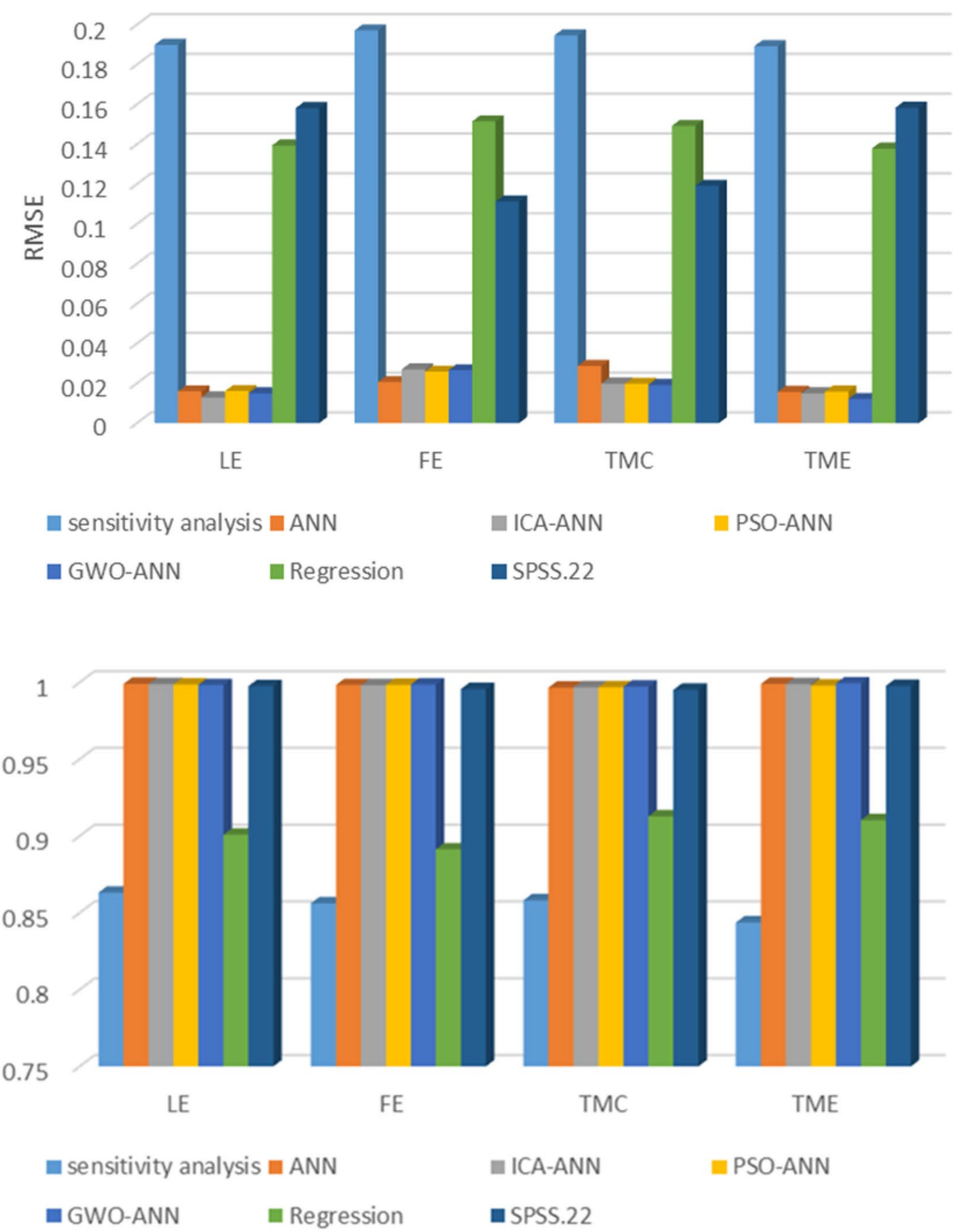

Fig. 9 Comparisons of **a** RMSE and **b** R^2 of the predictor algorithms using different statistical methods

models provide better results with regards to higher R^2 values and lower RMSE values.

As it can be seen, moisture content, swelling index, soil compressibility factor and type of soil have low effect on cost and energy consumption. On the other hand, in case of specific gravity, when specific gravity of ground becomes greater, weight of determined volume of the soil increases as well and work hours of machine for clearing specific surface is becoming higher and subsequently more fuel will be consumed. This goes in the same way for soil cut/fill volume. As soil cut/fill volume increases, work hours of machine and number of laborers increase as well and again more fuel will be consumed.

As it is clear, moisture content, swelling factor and type of soil, although less than other factors, have effects on energy consumption. Moisture content, soil compressibility factor and specific gravity in finetextured soils, like clays, and in soils with high organic materials lead to higher resistance against machine movement, which in turn adversely affect the energy consumption

Conclusion

Since a limited number of research related to energy consumption in land leveling has been done to measure the effects of soil and land properties, at this research, energy and cost of land leveling as a function of land characteristics have been evaluated. Studied characteristics of land in this research were: soil cut/fill volume, soil compressibility factor, specific gravity, moisture content, slope, sand percent, and soil swelling index. Based on these characteristics, artificial intelligence and computational methods such as ANN, and ICA-–ANN were used to determine the energy characteristics, i.e., FE, LE, TMC, TME. At this study, the ability of ANN, ICA–ANN, sensitivity analysis, regression, and ANFIS as well as PSO–ANN, GWO and SPSS for prediction of environmental indicators (LE, FE, TMC, and TME) during land leveling were investigated and compared. According to the results, 10-8-3-1, 10-8-2-5-1, 10-5-8-10-1, and 10-6-4-1 MLP network structures that were trained using Levenberg–Marquardt had the best performance. Sensitivity analysis revealed that only three variables including density, soil compressibility factor, and V had the highest effect on the output parameters including LE, FE, TMC and TME, and the accurate modes that relate each parameter to one another were extracted. Using regression method, only three variables including slope, V and SSI were determined to be effective on FE. Results approved the superiority of integrated methods, especially ICA–ANN, compared to other methods such as regression and statistical software such as SPSS and Minitab. Moreover, the ANFIS models with hybrid optimization method and Sugeno FIS type show better performance than the models based on back propagation and Mamdani techniques. All ANFIS-based models have R^2 values above 0.995 and MSE values below 0.002.

Based on the results, ANN and ICA–ANN algorithms are the most capable methods to predict LE and FE. In the same way, GWO–ANN was found to be more powerful and accurate in prediction of TMC and TME. In fact, comparing ANN, ICA–ANN, PSO–ANN, GWO–ANN and sensitivity analysis methods in estimating the amount of LE, FE, TMC and TME based on statistical indicators shows that GWO–ANN and ICA–ANN methods are more accurate, despite very slight difference between their results. On the other hand, sensitivity analysis method is the least accurate one. Ability of GWO–ANN and ICA–ANN models in prediction of sophisticated problems with high accuracy makes it a powerful tool for engineers and researchers to use it not only in agricultural operations, but also in other fields such as finance, mining, infrastructures, etc. Using this tool will lead to an economical land leveling operations in farm lands. These implications are consistent with the findings and conclusions of this study. Furthermore, implementing this technique on heavy operations such as land leveling will help in protecting the environment which in turn increases the life quality.

Abbreviations
GWO–ANN: Integrating Artificial Neural Network and Grey Wolf Optimizer (GWO); ICA–ANN: Integrating Artificial Neural Network and imperialist competitive algorithm; ANN: Artificial Neural Network; LE: environmental indicators: labor energy; FE: environmental indicators: fuel energy; TMC: total machinery cost; TME: environmental indicators: total machinery energy.

Authors' contributions
IA carried out all studies about the work and cultivated the data which were necessary to be analyzed. FM participated in land leveling studies results acquisition. SA helped in design and studying of artificial neural networks ANFIS and statistical analyses. All authors read and approved the final manuscript.

Author details
[1] Department of Surveying and Geometric Eng, Engineering Faculty, University of Tehran, Tehran, Iran. [2] College of Agriculture, University of Basrah, Basrah, Iraq. [3] College of Agriculture and Natural Resources, University of Tehran, Tehran, Iran.

Acknowledgements
We are thankful to our colleagues, faculty and Ph.D. students who helped us at Department of Surveying and Geometrics Engineering, and Department of Agriculture and Natural Recourses of the University of Tehran, Iran, who provided expertise that greatly assisted the research.

Competing interests
The authors declare that they have no competing interests.

Availability of data and materials
The dataset supporting the conclusions of this article will not be shared due to performing our next projects with this software.

Consent for publication
Not applicable.

Ethics approval and consent to participate
Not applicable.

Funding
All parts of this research have been supported by the University of Tehran.

Received: 20 January 2018 Accepted: 22 January 2019
Published online: 27 February 2019

References

1. Shakibai AR, Koochekzadeh S. Modeling and predicting agricultural energy consumption in Iran. Am-Eur J Agric. 2009;5(3):308–12.
2. Okasha EM, Abdelraouf RE, Abode MAA. Effect of land leveling and water applied methods on yield and irrigation water use efficiency of maize (*Zea mays* L.) grown under clay soil conditions. World Appl Sci J. 2013;27(2):183–90.
3. Brye KR, Slaton NA, Norman RJ. Soil physical and biological properties as affected by land leveling in a clayey aquent. Soil Sci Soc Am J. 2006;70(2):631–42.
4. McFarlane BL, Stump-Allen RCG, Watson DO. Public perceptions of natural disturbance in Canada's national parks: the case of the mountain pine beetle (Dendroctonus ponderosa Hopkins. Biolo Con. 2006;130(3):340–8.
5. Khan F, Khan SU, Sarir MS, Khattak RA. Effect of land leveling on some physico-chemical properties of soil in district dir lower. Shar J Agric. 2007;23(1):108–14.
6. Severino G, et al. The IoT as a tool to combine the scheduling of the irrigation with the geostatistics of the soils. Fut Gen Computer Syst. 2018;82:268–73.
7. Moghaddam K, Far T. Laser land levelling as a strategy for environmental management: the case of Iran. Pollution. 2015;1(2):203–15.
8. Toro J, Requena I, Zambrano M. Environmental impact assessment in Colombia: critical analysis and proposals for improvement. Environ Impact Asses. 2010;30(4):247–61.
9. Giannino F, et al. A predictive decision support system (DSS) for a microalgae production plant based on Internet of Things paradigm. Concurren Comput Prac Experience. 2018;30(15):e4476.
10. Diamantopoulou MJ. Artificial neural networks as an alternative tool in pine bark volume estimation. Comput Electron Agr. 2005;48:235–44.
11. Lei K, Qiu Y, He Y. A new adaptive well-chosen inertia weight strategy to automatically harmonize global and local search ability in particle swarm optimization. In: Systems and Control in Aerospace and Astronautics 2006. 1st international symposium on systems and control in aerospace and astronautics. 2006. IEEE
12. Ahmadi MA, Ahmadi MR, Shadizadeh SR. Evolving artificial neural network and imperialist competitive algorithm for prediction permeability of the reservoir. Appl Soft Comput. 2013;13(2):1085–98.
13. Ahmadi MA, Soleimani R, Bahadori A. A computational intelligence scheme for prediction equilibrium water dew point of natural gas in TEG dehydration systems. Fuel. 2014;137:145–54
14. Ahmadi MA, Golshadi M. Neural network based swarm concept for prediction asphaltene precipitation due to natural depletion. J Petrol Sci Eng. 2012;98:40–9.
15. Taghavifar H, Mardani A, Taghavifar L. A hybridized artificial neural network and imperialist competitive algorithm optimization approach for prediction of soil compaction in soil bin facility. Measurement. 2013;46(8):2288–99.
16. Ahmadi MA, Bahadori A, Shadizadeh SR. A rigorous model to predict the amount of dissolved calcium carbonate concentration throughout oil field brines: side effect of pressure and temperature. Fuel. 2015;139:154–9.
17. Fereydooni M, Mansoori J. Evaluation of multilayer perceptron models and adaptive neuro-fuzzy interference systems in the simulation of groundwater level (case study: lamer plain. Indian J Fundam Appl life Sci. 2015;5:1076–83.
18. Fereydooni M, Mansoori B. Simulation depth of bridge pier scouring using artificial neural network and adaptive neuro-fuzzy inference system. Indian J Fund Appl Life Sci. 2015;5:2091–5.
19. Nazari-Shirkouhi S, Eivazy H, Ghodsi R, Rezaie K, Atashpaz-Gargari E. Solving the integrated product mix-outsourcing problem using the imperialist competitive algorithm. Expert Syst Appl. 2010;37(12):7615–26.
20. Atashpaz-Gargari, E. and C. Lucas. Imperialist competitive algorithm: an algorithm foroptimization inspired by imperialistic competition. In: Evolutionary computation. CEC2007. IEEE Congress on; 2007. IEEE.
21. Abdechiri M, Faez K, Bahrami H. Adaptive Imperialist competitive algorithm (AICA). In: cognitive informatics (ICCI). 9th IEEE international conference. 2010. p. 940–945.
22. Ebrahimzadeh A, Addeh J, Rahmani Z. Control Chart Pattern Recognition Using K-MICA Clustering and Neural Networks. ISA Trans. 2012;51(1):111–9.
23. Rajabioun R, Atashpaz-Gargari E, Lucas C. Colonial competitive algorithm as a tool for nash equilibrium point achievement. In: International Conference on Computational Science andIts Applications. Springer; 2008.
24. Abdi B, Mozafari H, Ayob A, Kohandel R. Imperialist competitive algorithm and its application in optimization of laminated composite structures. Eur J Scl R. 2011;55(2):174–87.
25. Talatahari S, Kavehand A, Sheikholeslami R. Chaotic imperialist competitive algorithm for optimum design of truss structures. Str Multidiscip Optim. 2012;46(3):355–67.
26. Kaveh A, Talatahari S. Optimum design of skeletal structures using imperialist competitive algorithm. Comput Struct. 2010;88(21–22):1220–9.
27. Mohammadi A, Rafiee S, Keyhani A, Emam-Djomeh Z. Modelling of kiwifruit (cv.Hayward) slices drying using artificial neural network. In: 4th international conference on energy efficiency and agricultural engineering. Bulgaria: Rousse; 2009. p. 397–404.
28. Movagharnejad K, Nikzad M. Modeling of tomato drying using artificial neural network. Comput Electron Agr. 2007;59(1):78–85.
29. Cassel D, Wood M, Bunge RP, Classer L. Mitogenicity of brain axolemma membranes and soluble factors for dorsal root ganglion schwann cells. J Cell Biochem. 1982;18(4):433–45.
30. Tiryaki B. Predicting intact rock strength for mechanical excavation using multivariate statistics, artificial neural networks, and regression trees. Eng Geol. 2008;99(1–2):51–60.
31. Marto A, Hajihassani M, Armaghani D, Mohamad ED, Makhtar AM. A novel approach for blast-induced flyrock prediction based on imperialist competitive algorithm and artificial neural network. Sci World J. 2014;2014(15):1–11.
32. Azadeh A, Ghaderi SF, Sohrabkhani S. Annual electricity consumption forecasting by neural network in high energy consuming industrial sectors. Energy Convers Manage. 2008;49(8):2272–8.
33. Nikoo MF, Ramezani M, Hadzima-Nyarko E, Nyarko K, Nikoo M. Flood-routing modeling with neural network optimized by social-based algorithm. Nat Hazards. 2016;82(1):1–24.